Biointerface Research in Applied Chemistry
Open-Access Journal (ISSN: 2069-5837)

Article
Volume 13, Issue 6, 2023, 563
https://doi.org/10.33263/BRIAC136.563

Photoelectrode Properties Based on TiO_2 Photocatalyst Doped Non-Metallic Agent as Initial Model for Detection and Degradation of Pesticide Pollutants

Zul Arham [1], Andi Khaeruni Ramli [2], Muhammad Natsir [3], Muhammad Nurdin [3,*]

[1] Doctoral Student, Study Program of Agricultural Science, Post Graduate School, Universitas Halu Oleo, Kendari 93232 – Southeast Sulawesi, Indonesia
[2] Department of Plant Protection, Faculty of Agriculture, Universitas Halu Oleo, Kendari 93232 – Southeast Sulawesi, Indonesia
[3] Department of Chemistry, Faculty of Mathematics and Natural Sciences, Universitas Halu Oleo, Kendari 93232 – Southeast Sulawesi, Indonesia
* Correspondence: mnurdin06@yahoo.com; (M.N.);

Scopus Author ID 56678695400
Received: 29.11.2022; Accepted: 13.01.2023; Published: 19.03.2023

Abstract: A unique study has been carried out to determine the characteristics of a TiO2 photoelectrode modified with a non-metallic agent. The photoelectrode is designed for the initial model of the pesticide pollutant detection and degradation system. Wherein the non-metallic agent used in this investigation is a sulfur compound. The preparation of the TiO_2 photoelectrode used the principle of electrolysis with a potential bias of 25.0 V. Furthermore, and the photoelectrode was modified using a dip-coating technique. Result of XRD analysis showed that the crystallinity of TiO_2 anatase with a 2θ value of 25.5; 36.98; 37.50; 47.89; 53.97; 55.52; 62.74; 62.28; 62.70 and 69.71º. Morphology has observed the nanopore-shaped structures and presented the total amount of Ti, O, and S atoms in the composite were 51.44%, 43.46%, and 5.11%, respectively. The results of the FTIR analysis showed that there were S-O bonds that occurred at wave numbers 1153 cm^{-1} and 1116 cm^{-1}. In addition, based on this analysis shows that there is a Ti-O bond that occurs at wave number 1039 cm^{-1}. Overall this work demonstrates the potential of non-metallic agents for wider application as dopant TiO_2 photoelectrode for pesticide pollutant detection and degradation systems.

Keywords: TiO_2 photoelectrode; non-metallic doping; a sulfur compound; initial model.

1. Introduction

Technological advances have developed rapidly to support human life, especially in the textile and agricultural industries. This condition is seen as an opportunity to continue synthesizing chemicals that can be applied to both fields [1,2]. Pesticides are one of the chemical compounds that are currently being produced and used in agriculture. Pesticides are considered effective in eradicating and controlling pests and plant diseases. Even so, the number of uses that continues to increase is a new problem for plants, crop products, and the environment [3,4].

In addition to the detection model, the pesticide molecule degradation model continues to be developed. Models for detecting and degrading pesticide molecules based on photocatalyst materials are interesting to develop. In the electrometry-based detection model, photocatalyst materials such as TiO_2 effectively increase the electron transfer activity on the

surface of the electrode [5]. This condition makes the resulting peak current better. As for the degradation based on photoelectrocatalysis, the photocatalyst material shows very good pollutant degradation activity. This activity is indicated by a short degradation time and a long recombination rate [6]. Based on this, the photocatalyst-based detection and degradation method is a new method suitable for environmental applications [7]. Among other semiconductor materials such as ZnO, Fe_2O_3, $FeTiO_3$, Al_2O_3, and Cu_2O, TiO_2 is reported to have an attractive performance for application in photocatalytic systems. TiO_2 has high sensitivity, good oxidation-reduction properties, and is stable, inert, and environmentally friendly. TiO2, anatase, and rutile crystal structure is reported to have very good activity. The very strong redox properties of TiO_2 photocatalysts occur when the surface is irradiated with ultraviolet (UV) light at a wavelength (λ) of 365-385 nm [8,9]. TiO_2 irradiation causes electron excitation resulting in a positive hole in the valence band (Vb). The positive hole (h^+) is a strong oxidizing agent with a potential value of 2.8 volts [10]. At the same time, irradiating TiO_2 causes the formation of reducing agents, which will form superoxide radicals and hydrogen peroxide.

To improve the performance of TiO_2 photocatalysts, researchers have reported using TiO_2-coated Ti plates as photoelectrodes. TiO_2-coated Ti (TiO_2/Ti) functions as working electrodes in detecting and degrading pesticide pollutants. Photoelectrodes describe a much better degradation activity when compared to the use of TiO_2 powder. The recombination of electron-hole pairs can be controlled through the external circuit of the photoelectrode system. Another effort that has also been reported in controlling the rate of electron-hole pairs is by doping photoelectrodes using several non-metallic dopants, such as C [11], S [12,13], N [14], F [15], P [16], and B [17].

Based on the above problems, we report the potential of sulfur as a non-metallic dopant for TiO_2/Ti photoelectrodes. Sulfur attracted our attention because of its good photocatalytic activity, thermal stability, and reduced band gap of TiO_2.

2. Materials and Methods

2.1. Materials.

The materials used in this study were Ti plate (purity level of 99% with a thickness of 0.5 mm), titanium isopropoxide, TTIP (purity level > 97%), acetylacetone (Merck), ethanol (Merck, 98%), hydrochloric acid, acetate (Merck), ammonium chloride (Merck), copper plate (Cu), nitric acid (Merck), hydrofluoric acid (Merck), ammonium fluoride (Merck), sodium nitrate, glycerol (pa), and distilled water.

2.2. Synthesis of TiO_2/Ti photoelectrode.

The Ti plate was inserted into the probe containing a mixture of 0.27 M NH_4F solution, distilled water, and glycerol. The anodization process is carried out by placing a Titanium plate as the anode and a Cu plate as the cathode. This process uses a potential of 25 volts and is carried out for four hours. After obtaining the TiO_2/Ti photoelectrode, the photoelectrode was then calcined for 1.5 hours at 500ºC to evaporate the remaining electrolyte solution and obtain TiO_2 anatase crystals with better activity than other types of crystals [18].

2.3. Synthesis of TiO_2/Ti-doped sulfur.

The synthesis of TiO_2/Ti-doped sulfur was carried out in two stages, namely sol-gel, and dip-coating. The sol-gel stage aims to obtain sulfur-doped TiO_2 (S-TiO_2). In this case, sulfuric acid is used as a sulfur agent. The dip-coating stage aims to coat the surface of the TiO_2/Ti photoelectrode with the S-TiO_2 suspension obtained in the sol-gel stage. The dip-coating stage lasted 10 minutes. After that, the photoelectrode was slowly removed and calcined at 200°C for 15 minutes. An illustration of the synthesis process is shown in Figure 1.

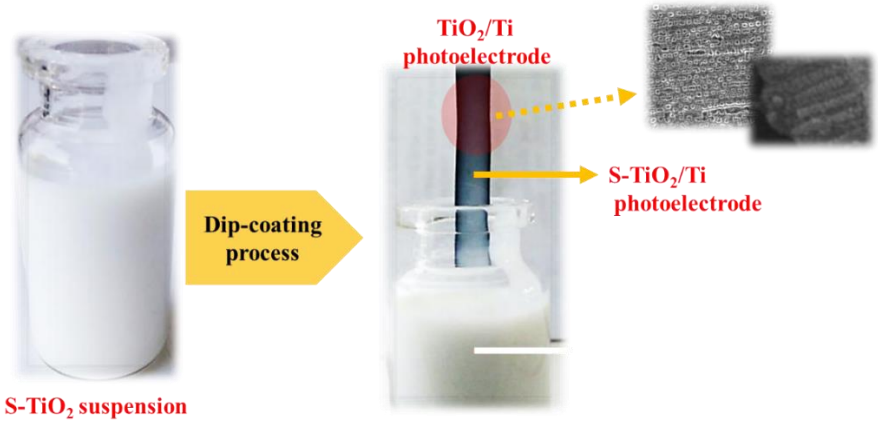

Figure 1. Illustration of the S-TiO_2/Ti photoelectrode synthesis process.

2.4. Test the characteristics of TiO_2/Ti and S-TiO_2/Ti photoelectrodes.

The characteristics of the photoelectrodes, both TiO_2/Ti and S-TiO_2/Ti, were carried out using a 3-electrode-based Linear Sweep Voltammetry (LSV) technique. The photoelectrodes (TiO_2 and S-TiO_2) were placed as working electrodes, Ag/AgCl as reference electrodes, and platinum wire was placed as auxiliary electrodes. The potential range used is ± 1.0 volts at a scan rate of 100 mV. The test was carried out on a 0.1 M KNO_3 electrolyte solution in the presence of UV and Visible light.

3. Results and Discussion

3.1. Photoelectrode synthesis of TiO_2 and S-TiO_2.

The anodizing process carried out the synthesis of TiO_2 for 4 hours with a potential bias of 25.0 Volt [2]. Potential bias giving will cause Ti^{4+} ions to migrate from Ti metal to electrolyte and combine with F^- ions to form the titanium hexafluoride complex $[TiF_6]^{2-}$ [26]. The presence of anions such as O^{2-} and -OH results from water decomposition and will migrate with the F^- ion toward the anode. The interaction of titanium with O^{2-} and -OH ions cause oxide growth on the metal surface can be seen in (Figure 2a). F^- ion, which migrates towards the anode, will destroy the oxide layer that has been formed to produce a tubular shaft [19]. The anodization of titanium in the fluoride ion-containing electrolytes can be ascribed to a competition between the following two chemical reactions [20]:

$$Ti + 2H_2O \quad TiO_2 + 4H^+ + 4e^-$$

$$TiO_2 + 6F^- + 4H^+ \quad [TiF_6]_2^- + 2H_2O$$

Figure 2b shows the sol-gel filled on the TiO_2 surface. The sol-gel that was used from Titanium Isopropoxide (TTIP) functions as a matrix or the distribution media of ionic dopant. Visually it seemed that the TiO_2 photoelectrode was coated by the sol-gel.

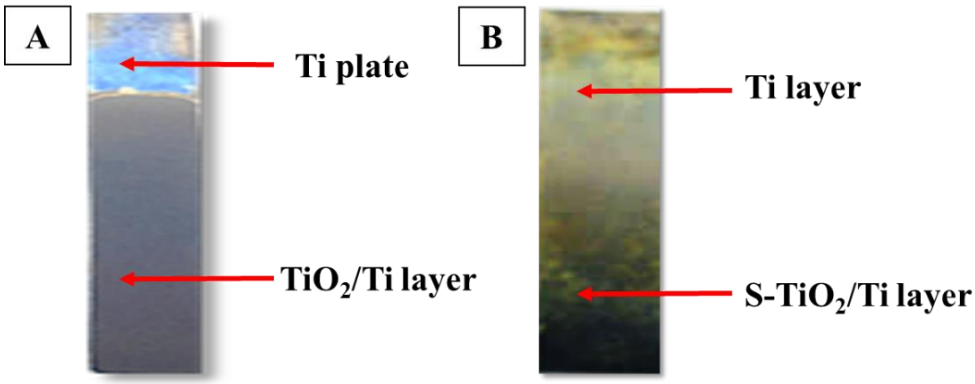

Figure 2. The results of photoelectrodes: **(a)** TiO_2, **(b)** TiO_2@S.

3.2. X-ray diffraction (XRD) characterization.

The X-ray diffraction pattern of TiO_2 photoelectrode is shown in Figure 3. It is noted that all the diffraction peaks represented the anatase phase with the characteristic high-intensity peak at 2θ around 25.5º (011), 36.98º (013), 37.50º (004), 47.89º (020), 53.97º (015), 55.2º (121), 62.28º (123), 62.70º (024), and 69.71º (220). These results have been confirmed with Crystallography Open Database (COD) numbers [96-720-6076], [96-500-0224] & [96-101-0943] [21]. The anatase TiO_2 has the smallest effective mass averaged (e^-/h^+) compared with the rutile and brookite. The small effective mass allowed electrons to quickly migrate to the surface of TiO_2 particles so that the photogeneration recombination rate in the anatase TiO_2 of smaller [22].

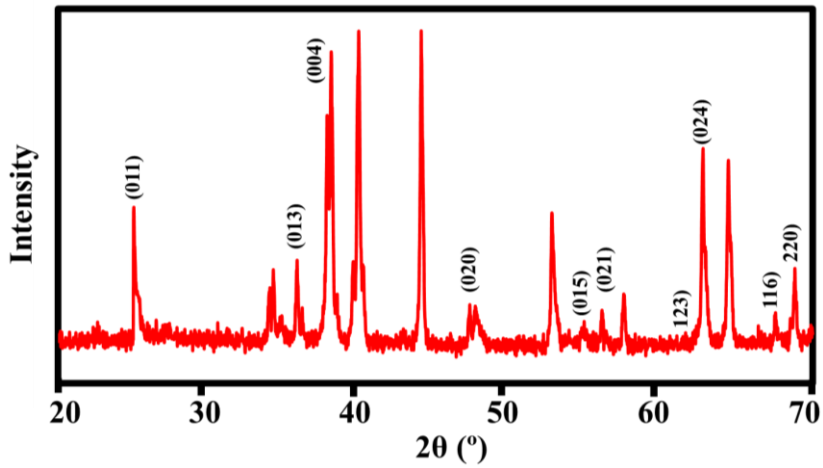

Figure 3. The XRD pattern of TiO_2 photoelectrode.

3.3. Fourier Transform Infra-Red (FTIR) characterization.

Figure 4 illustrates the FTIR spectra of TiO_2@S photoelectrode. It was observed that three absorption peaks were located at wavenumber 3412 cm^{-1}, 1039 cm^{-1}, 1153 cm^{-1}, and 1116 cm^{-1}. The peak located at 3412 cm^{-1} was indicated to correspond to a hydroxyl group (O-H) stretching with a stronger peak [23]. The presence of the O-H group is indicated to correspond with the titanyl group as Ti-OH from the crystalline phase of TiO_2 and water absorbed on the surface of TiO_2 [24]. The peak at 1039 cm^{-1} was assigned to Ti-O stretching vibration. The peak at 1153 cm^{-1} and 1116 cm^{-1} corresponded to S-O bond stretching vibration. The formation of the S-O bond was indicated by sulfur as a dopant that binds to one of the oxygen atoms from TiO_2 [25].

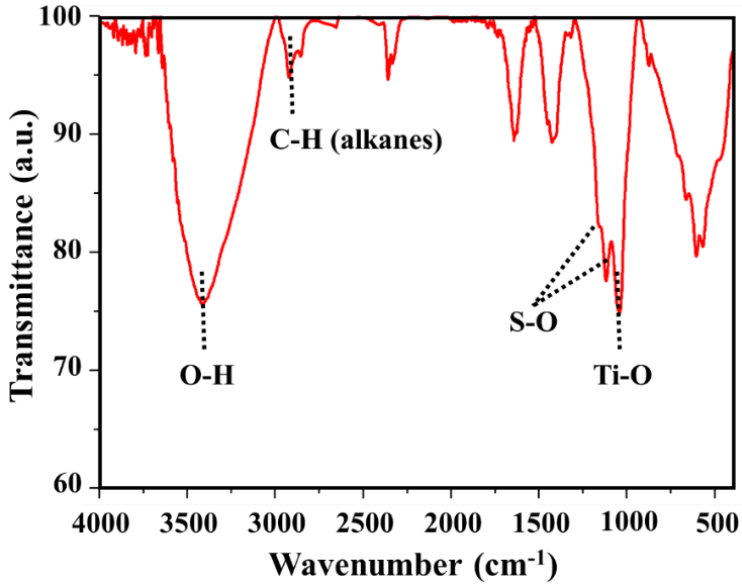

Figure 4. IR spectra of S-TiO_2 photoelectrode.

3.3. SEM-EDX characterization.

The morphology and size of TiO_2 and S-TiO_2 photoelectrodes were characterized by Scanning Electron Microscopy (SEM). Figure 5a shows the formation of a shaft in the form of a tube, and the presence of pores on the electrode surface indicates it. At the same time, Figure 5b shows a fine layer that is spread evenly on the surface of the electrode, which indicates the attachment of S-TiO_2 sol-gel on the TiO_2 photoelectrode. At a magnification of 500 nm, there is a gap in the TiO_2 layer, probably due to the high heating during the dip-coating process. On the other hand, gaps allow organic molecules to be adsorbed on the surface of TiO_2 photoelectrode [15].

Further, to verify the existence of S, the Energy Dispersive X-ray (EDX) spectra of TiO_2 photoelectrode are shown in Figure 5c. From the EDX spectra, the elements Ti, O, and S were observed in the samples that have been synthesized. As seen in Figure 5c, the presentation of sulfur (S) at TiO_2 is 5.11%. These results indicate the success of S doping on TiO_2.

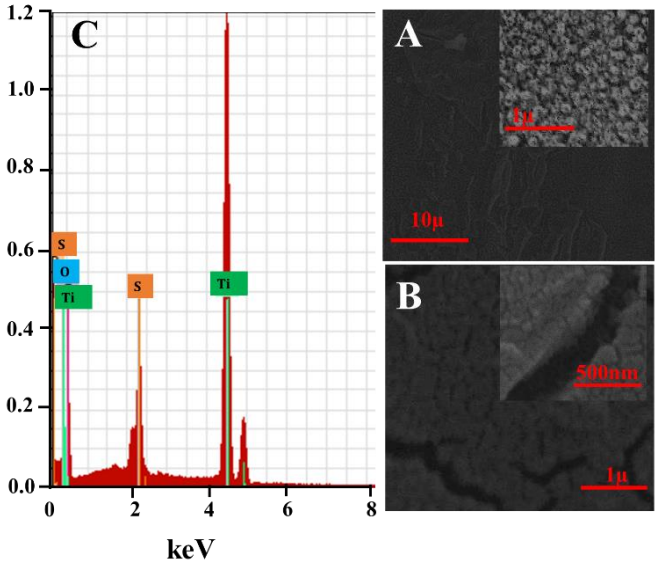

Figure 5. Surface morphology of photoelectrodes: **(A)** TiO_2; **(B)** S-TiO_2; and **(C)** EDX results of S-TiO_2 photoelectrodes.

3.4. Electrochemical characteristics of the photoelectrode.

The photoelectrochemical activity was observed by the Linear Sweep Voltammetry (LSV) method based on current (I) measurement as the potential function (V) [26–28]. Based on Figure 6a showed the highest TiO_2 photoelectrode activity at the time of UV light irradiation because TiO_2 had photoelectrocatalysis activities on the irradiation of UV light with a wavelength ≤ 388 nm and energy gap of 3.2 eV [9]. Whereas the irradiation with visible light and without irradiation (dark) did not show good activity in the measurement process, this was because the visible light had a wavelength greater than the energy given, so it was very difficult to be absorbed by the TiO_2 photoelectrode, and in the dark condition, the TiO_2 photoelectrode did not produce the energy that would be transmitted from the conduction band to the valence band [29]. Figure 6b shows the good performance of S-TiO_2 photoelectrode when it was radiated by UV light. The irradiation using visible light had better activity than UV light because of the addition of non-metallic sulfur on the surface of TiO_2 photoelectrodes capable of shifting the conduction band. Therefore S-TiO_2 photoelectrodes can reduce electron recombination and hole.

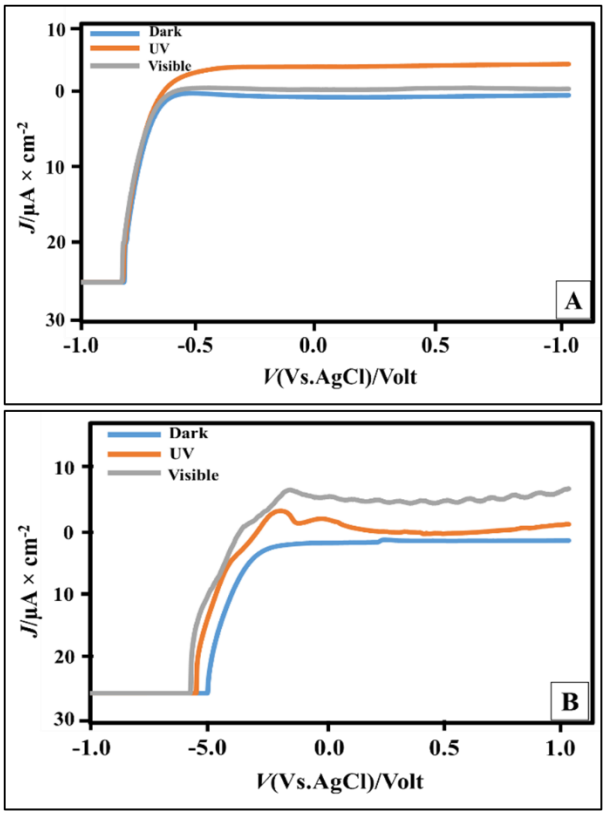

Figure 6. LSV voltammogram: **(a)** TiO_2 photoelectrode; **(b)** S-TiO_2 photoelectrode.

4. Conclusions

In general, the characteristics of S-TiO_2-based photoelectrodes have been studied in this work. The photoelectrode was synthesized in several stages, including anodizing a titanium plate to obtain a TiO_2 photoelectrode, sol-gel to obtain S-TiO_2, and dip-coating to obtain a TiO_2 photoelectrode coated with S-TiO_2. The characterization results, XRD, FTIR, and SEM-EDX, show the success of the photoelectrode synthesis process. The results of electrochemical characterization using Linear Sweep Voltammetry (LSV) showed that the S-TiO_2-coated TiO_2 photoelectrode produced a better current response than the unmodified photoelectrode. These

results indicate the potential of non-metallic agents for wider application as dopant TiO_2 photoelectrodes.

Funding

This research was funded by the Ministry of Education, Culture, Research and Technology of the Republic of Indonesia under the Doctoral Dissertation Research award grant no 44/UN29.20/PG/2022 and SP-DIPA-023.17.1.690523/2022

Acknowledgments

We acknowledge our gratitude for the financial support from the Ministry of Education, Culture, Research and Technology of the Republic of Indonesia through the Doctoral Dissertation Research Program from 2022 to 2023.

Conflicts of Interest

The authors declare no conflict of interest.

References

1. Natsir, M.; Putri, Y.I.; Wibowo, D.; Maulidiyah, M.; Salim, L.O.A.; Azis, T.; Bijang, C.M.; Mustapa, F.; Irwan, I.; Arham, Z. Effects of Ni–TiO_2 pillared Clay–Montmorillonite composites for photocatalytic enhancement against reactive orange under visible light. *Journal of Inorganic and Organometallic Polymers and Materials* **2021,** *31*, 3378–3388, https://doi.org/10.1007/s10904-021-01980-9.
2. Arham, Z.; Kurniawan, K.; Ismaun, I. Synthesis of TiO_2 Photoelectrode Nanostructures for Sensing and *Removing Textile Compounds Rhodamine B.* **2021,** *12*, 5479-5485, https://doi.org/10.33263/BRIAC124.54795485.
3. Nurdin, M.; Prabowo, O.A.; Arham, Z.; Wibowo, D.; Maulidiyah, M.; Saad, S.K.M.; Umar, A.A. Highly sensitive fipronil pesticide detection on ilmenite (FeO. TiO_2)-carbon paste composite electrode. *Surfaces and Interfaces* **2019,** *16*, 108–113, https://doi.org/10.1016/j.surfin.2019.05.008.
4. Nurdin, M.; Arham, Z.; Rasyid, J.; Maulidiyah, M.; Mustapa, F.; Sosidi, H.; Ruslan, R.; Salim, L.O.A. Electrochemical performance of carbon paste electrode modified TiO_2/Ag-Li (CPE-TiO_2/Ag-Li) in determining fipronil compound. In Proceedings of the *Journal of Physics: Conference Series; IOP Publishing* **2021**, *1763*, 12067, http://doi.org/10.1088/1742-6596/1763/1/012067.
5. Nurdin, M.; Arham, Z.; Irna, W.O.; Maulidiyah, M.; Kurniawan, K.; Irwan, I.; Umar, A.A. Enhanced-charge transfer over molecularly imprinted polyaniline modified graphene/TiO_2 nanocomposite electrode for highly selective detection of fipronil insecticide. *Materials Science in Semiconductor Processing* **2022,** *151*, 106994, https://doi.org/10.1016/j.mssp.2022.106994.
6. Nurdin, M.; Muzakkar, M.Z.; Maulidiyah, M.; Trisna, T.; Arham, Z.; La Salim, O.A.; Irwan, I.; Umar, A.A. High-Performance COD Detection of Organic Compound Pollutants using Sulfurized-TiO_2/Ti Nanotube Array Photoelectrocatalyst. *Electrocatalysis* **2022,** 1–10, https://doi.org/10.1007/s12678-022-00746-2.
7. Azis, T.; Nurdin, M.; Riadi, L.S.; Arham, Z.; Irwan, I.; Salim, L.O.A.; Maulidiyah, M. Photoelectrocatalytic performance of ilmenite ($FeTiO_3$) doped TiO_2/Ti electrode for reactive green 19 degradation in the UV-visible region. *In Proceedings of the Journal of Physics: Conference Series; IOP Publishing* **2021**, *1899*, 12041, http://doi.org/10.1088/1742-6596/1899/1/012041.
8. Nurdin, M.; Wibowo, D.; Azis, T.; Safitri, R.A.; Maulidiyah, M.; Mahmud, A.; Mustapa, F.; Ruslan, R.; Salim, A.; Ode, L. Photoelectrocatalysis Response with Synthetic Mn–N–TiO_2/Ti Electrode for Removal of Rhodamine B Dye. *Surface Engineering and Applied Electrochemistry* **2022,** *58*, 125–134, https://doi.org/10.3103/S1068375522020077.
9. Wibowo, D.; Nurdin, M. Determination of COD based on Photoelectrocatalysis of $FeTiO_3$.TiO_2/Ti Electrode. *In Proceedings of the IOP Conference Series: Materials Science and Engineering; IOP Publishing* **2017**, *267*, 12007, http://doi.org/10.1088/1757-899X/267/1/012007.
10. Shandilya, P.; Raizada, P.; Singh, P. Photocatalytic degradation of azo dyes in water. In *Water Pollution and Remediation: Photocatalysis*, **2021**, 119–146, https://doi.org/10.1007/978-3-030-54723-3.
11. He, X.; Wu, M.; Ao, Z.; Lai, B.; Zhou, Y.; An, T.; Wang, S. Metal–organic frameworks derived C/TiO_2 for visible light photocatalysis: Simple synthesis and contribution of carbon species. *Journal of Hazardous Materials* **2021,** *403*, 124048, https://doi.org/10.1016/j.jhazmat.2020.124048.
12. Helmy, E.T.; Abouellef, E.M.; Soliman, U.A.; Pan, J.H. Novel green synthesis of S-doped TiO_2 nanoparticles

using Malva parviflora plant extract and their photocatalytic, antimicrobial and antioxidant activities under sunlight illumination. *Chemosphere* **2021,** *271*, 129524, https://doi.org/10.1016/j.chemosphere.2020.129524.
13. Tariq, F.; Hussain, R.; Noreen, Z.; Javed, A.; Shah, A.; Mahmood, A.; Sajjad, M.; Bokhari, H.; ur Rahman, S. Enhanced antibacterial activity of visible light activated sulfur-doped TiO_2 nanoparticles against Vibrio cholerae. *Materials Science in Semiconductor Processing* **2022,** *147*, 106731, https://doi.org/10.1016/j.mssp.2022.106731.
14. Mersal, M.; Mohamed, G.G.; Zedan, A.F. Promoted visible-light-assisted oxidation of methanol over N-doped TiO_2/WO_3 nanostructures. *Optical Materials* **2021,** *122*, 111810, https://doi.org/10.1016/j.optmat.2021.111810.
15. Liu, D.; Tian, R.; Wang, J.; Nie, E.; Piao, X.; Li, X.; Sun, Z. Photoelectrocatalytic degradation of methylene blue using F doped TiO_2 photoelectrode under visible light irradiation. *Chemosphere* **2017,** *185*, 574–581, https://doi.org/10.1016/j.chemosphere.2017.07.071.
16. Zhan, X.; Zhao, Y.; Zhou, G.; Yu, J.; Wang, H.; Shi, H. Oxygen-containing groups and P doped porous carbon nitride nanosheets towards enhanced photocatalytic activity. *Chemosphere* **2022,** *287*, 132399, https://doi.org/10.1016/j.chemosphere.2021.132399.
17. da Silva, T.F.; Cavalcante, R.P.; Guelfi, D.R.V.; de Oliveira, S.C.; Casagrande, G.A.; Caires, A.R.L.; de Oliveira, F.F.; Gubiani, J.R.; Cardoso, J.C.; Junior, A.M. Photo-anodes based on B-doped TiO_2 for photoelectrocatalytic degradation of propyphenazone: Identification of intermediates, and acute toxicity evaluation. *Journal of Environmental Chemical Engineering* **2022,** *10*, 107212, https://doi.org/10.1016/j.jece.2022.107212.
18. Nurdin, M. Maulidiyah. Fabrication of TiO_2/Ti nanotube electrode by anodizing method and its application on photoelectrocatalytic system. *International Journal of Scientific & Technology Research* **2014,** *3*, 122–124, https://www.ijsr.net/allvolumes.php.
19. Regonini, D.; Bowen, C.R.; Jaroenworaluck, A.; Stevens, R. A review of growth mechanism, structure and crystallinity of anodized TiO_2 nanotubes. *Materials Science and Engineering: R: Reports* **2013,** *74*, 377–406, https://doi.org/10.1016/j.mser.2013.10.001.
20. Okada, M.; Tajima, K.; Yamada, Y.; Yoshimura, K. Self-organized formation of short TiO_2 nanotube arrays by complete anodization of ti thin films. *Physics Procedia* **2012,** *32*, 714–718, https://doi.org/10.1016/j.phpro.2012.03.622.
21. Niu, H.; Wang, Q.; Liang, H.; Chen, M.; Mao, C.; Song, J.; Zhang, S.; Gao, Y.; Chen, C. Visible-light active and magnetically recyclable nanocomposites for the degradation of organic dye. *Materials* **2014,** *7*, 4034–4044, http://doi.org/10.3390/ma7054034.
22. Zhang, J.; Zhou, P.; Liu, J.; Yu, J. New understanding of the difference of photocatalytic activity among anatase, rutile and brookite TiO_2. *Physical Chemistry Chemical Physics* **2014,** *16*, 20382–20386, https://doi.org/10.1039/C4CP02201G.
23. Lin, Y.-H.; Hsueh, H.-T.; Chang, C.-W.; Chu, H. The visible light-driven photodegradation of dimethyl sulfide on S-doped TiO_2: Characterization, kinetics, and reaction pathways. *Applied Catalysis B: Environmental* **2016,** *199*, 1–10, https://doi.org/10.1016/j.apcatb.2016.06.024.
24. Jagadale, T.C.; Takale, S.P.; Sonawane, R.S.; Joshi, H.M.; Patil, S.I.; Kale, B.B.; Ogale, S.B. N-doped TiO_2 nanoparticle based visible light photocatalyst by modified peroxide sol− gel method. *The journal of physical chemistry C* **2008,** *112*, 14595–14602, https://doi.org/10.1021/jp803567f.
25. Nam, S.-H.; Kim, T.K.; Boo, J.-H. Physical property and photo-catalytic activity of sulfur doped TiO_2 catalysts responding to visible light. *Catalysis Today* **2012,** *185*, 259–262, https://doi.org/10.1016/j.cattod.2011.07.033.
26. Nurdin, M.; Azis, T.; Maulidiyah, M.; Aladin, A.; Hafid, N.A.; Salim, L.O.A.; Wibowo, D. Photocurrent responses of metanil yellow and remazol red b organic dyes by using TiO_2/Ti electrode. *In Proceedings of the IOP Conference Series: Materials Science and Engineering; IOP Publishing*, **2018**, 367, 12048, https://doi.org/10.1088/1757-899X/367/1/012048.
27. Maulidiyah, M.; Azis, T.; Lindayani, L.; Wibowo, D.; Salim, L.O.A.; Aladin, A.; Nurdin, M. Sol-gel TiO_2/Carbon Paste Electrode Nanocomposites for Electrochemical-assisted Sensing of Fipronil Pesticide. *Journal of Electrochemical Science and Technology* **2019,** *10*, 394–401, https://doi.org/10.33961/jecst.2019.00178.
28. Belháčová, L.; Krýsa, J.; Geryk, J.; Jirkovský, J. Inactivation of microorganisms in a flow-through photoreactor with an immobilized TiO_2 layer. *Journal of Chemical Technology & Biotechnology: International Research in Process, Environmental & Clean Technology* **1999,** *74*, 149–154, https://doi.org/10.1002/(SICI)1097-4660(199902)74:2<149::AID-JCTB2>3.0.CO;2-Q.
29. Azis, T.; Nurwahidah, A.T.; Wibowo, D.; Nurdin, M. Photoelectrocatalyst of Fe co-doped N-TiO_2/Ti nanotubes: pesticide degradation of thiamethoxam under UV–visible lights. *Environmental nanotechnology, monitoring & management* **2017,** *8*, 103–111, http://doi.org/10.1016/j.enmm.2017.06.002.